Available online at www.sciencedirect.com
SCIENCE DIRECT®
Journal of Molecular Catalysis A: Chemical 220 (2004) 221–228
JOURNAL OF MOLECULAR CATALYSIS A: CHEMICAL
www.elsevier.com/locate/molcata

A theoretical study of amines adsorption in HMOR by using ONIOM2 method

Nan Jiang [a], Shuping Yuan [a,*], Jianguo Wang [a], Haijun Jiao [a,b,1], Zhangfeng Qin [a], Yong-Wang Li [a]

[a] *State Key Laboratory of Coal Conversion, Institute of Coal Chemistry, Chinese Academy of Sciences, P.O. Box 165, Taiyuan 030001, PR China*
[b] *Leibniz-Institut für Organische Katalyse an der Universität Rostock e.V., Buchbinderstrasse 5-6, 18055 Rostock, Germany*

Received 24 December 2003; received in revised form 27 May 2004; accepted 27 May 2004

Abstract

The two-layered ONIOM method is used to study the interaction of amines (NH_3, $MeNH_2$, Me_2NH and Me_3N) with H-type mordenite (HMOR). For all the calculations, the high-layer is described by the B3LYP/6-31G(d,p) method, while the HF/3-21G method is used for the low-layer. In the adsorption complexes, proton transfer from the HMOR framework to amines is observed, and the protonated amines (R_3NH^+) are stabilized by hydrogen bonding between the negatively charged zeolite framework and the N–H bonds. The strength of the O···H–N hydrogen bonding is reflected by differences in the N–H stretching frequency of R_3NH^+ between the adsorbed state and the gas phase. The relative order of the amine basicity on the basis of the computed adsorption energies agrees well with the experiments, but differs from those in the gas phase (proton affinity) and in solvents (pK_a).

Keywords: Adsorption; Amines; HMOR; IR frequency; ONIOM2

1. Introduction

Zeolites play an important role as catalysts in petrochemical industry due to their Brønsted acidity and shape-selectivity. Temperature-programmed desorption and infrared (IR) experiments using NH_3 [1,2] and pyridine [3,4] as probes have been often carried out to characterize the acidity of zeolites. Theoretically, the interaction of molecules with the acid site in zeolites has attracted much attention because this is the initial step of chemical reactions catalyzed by acidic zeolites. Many studies were carried out to analyze the interactions of the Brønsted sites with a wide range of probes such as CO [5–7], NH_3 [8–10], CH_3OH [11–13], and H_2O [14,15]. For the interaction of NH_3 with the acid site in zeolites, for example, the proton transfer has been observed and NH_3 is transferred into NH_4^+ [10], which is stabilized by one or more hydrogen bonds between its hydrogen atoms and the oxygen atoms of the zeolite framework.

Mordenite (MOR) is a particularly useful catalyst for several applications including cracking and isomerization of hydrocarbons, dewaxing of heavy petroleum fractions and conversion of methanol to hydrocarbons [16]. As shown in Fig. 1, MOR has a structure of 12-membered ring channel interconnected by 8-membered side pockets. In the unit cell, there are ten different oxygen sites (from O_1 to O_{10}) and four tetrahedral sites (T_1, T_2, T_3 and T_4).

Earlier theoretical studies [17,18] showed that Al preferes T_4 site when replacing Si in MOR famework. In a recent work [19], we studied the adsorption of NH_3 on a HMOR cluster containing 8 tetrahedral sites (8T) and found that NH_3 becomes NH_4^+, and that there are three N–H···O hydrogen bonds between the [ZeO^-···NH_4^+] ion-pair. The successive replacement of hydrogen atoms in NH_3 by methyl groups can produce three amines ($MeNH_2$, Me_2NH and Me_3N) with enhanced basicity and bulky structures, which are expected to have different types and strength of interactions with the zeolite framework. Experimentally, Su and co-workers [20,21] studied the interaction of $MeNH_2$ with

* Corresponding author. Tel.: +86-351-4161578; fax: +86-351-4161578.
E-mail addresses: iccjgw@sxicc.ac.cn (S. Yuan), haijun.jiao@ifok.uni-rostock.de (H. Jiao).
[1] Fax: +49-381-4669324.

1381-1169/$ – see front matter © 2004 Elsevier B.V. All rights reserved.
doi:10.1016/j.molcata.2004.05.035

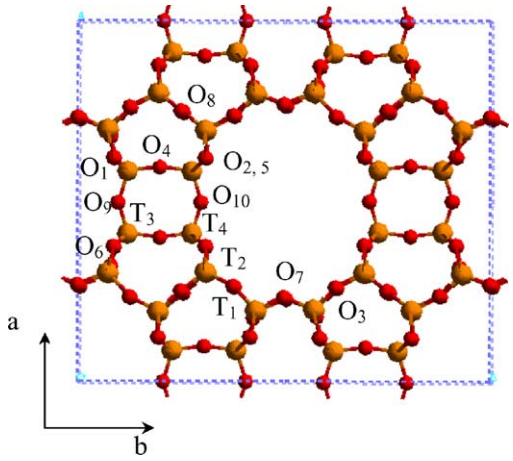

Fig. 1. The structure of mordenite unit-cell viewed down the *c*-axis (T_1, T_2, T_3, T_4, and O_1 to O_{10} are designated. Note that O_2 and O_5 sites are superposed in a projection along the *c*-axis).

several alkali cation exchanged large pore zeolites by IR and found that there are three types of interactions between $MeNH_2$ and the zeolite framework. The first one is the electronic interaction between the nitrogen lone pair of $MeNH_2$ and the counterions of the zeolite framework, which dominates the overall strength of the interaction. The two others are hydrogen-bonding type between the oxygen atoms of zeolite and the hydrogen atoms of the amine and methyl groups of $MeNH_2$. They claimed that it was the first time to observe and identify such interaction experimentally.

In order to satisfactorily model the pore structure of zeolites in which the adsorbates can be hold, large clusters are needed. However, accurate calculations of large clusters are very expensive or impractical. An effective solution to this problem is the embedding methods [22,10], in which the combination of quantum mechanical and molecular mechanical (QM/MM) methods are frequently used to simulate the zeolite frameworks and their interaction with other molecules [23,24]. The ONIOM method, developed by Morokuma and co-workers [25–27] and implemented in the Gaussian 98 [28] program, is one of the widespread QM/QM and QM/MM hybrid method suited for large-scale systems. In the ONIOM method, a large system can be partitioned into several layers, described at different levels of theory. Thus, an important feature of the ONIOM method is that it can describe the active center accurately at a high level and other less important parts at low levels of theory, and this method is especially useful when applied to large systems [29]. Roggero et al. [30] have successfully used the ONIOM method to model the adsorption of NH_3 at the isolated hydroxyl groups on a highly dehydrated silica surface. It was also applied successfully to study the catalytic reactions on HZSM-5 [31]. In this work, we report a study on the adsorption of a series of amines including NH_3, $MeNH_2$, Me_2NH and Me_3N in HMOR by using the two-layered ONIOM method (ONIOM2). The structures of the adsorption complexes are obtained, and the adsorption energies as well as IR frequencies are calculated to compare with the experimental data. The objective is to correlate the type and strength of interaction of HMOR with different adsorbates. By comparing the results of different amines with that of ammonia, it is desired to develop new molecular probes for the simultaneous characterization of acidity and basicity of zeolites.

2. Models and methods

2.1. Models

The coordination of the atoms in this work is taken from the structure of Na-MOR [32], which has a multiple pore-system with main channels of 12-membered rings that are connected by 8-membered ring channals. The 20T cluster model employed to represent the acid site and the pore structure of the MOR framework is shown in Fig. 2, which includes 20 tetrahedron centers and contains a complete 12-membered ring. In this cluster an Al atom replaces the Si atom at the T_4 site. To maintain the charge neutrality of the cluster, a charge-balancing proton is produced. The proton was initially put in a position where it is almost the same distance from the three oxygen atoms around the Al center (see Fig. 2a-1 and b-1). After the optimization, it is attached to O_{10} (see Fig. 2a-2 and b-2). Thus, it can be indicated that O_{10} is the energetically preferred position for the charge-balancing proton. This is also in agreement with our earlier study [18]. Each peripheral oxygen atoms in the clusters is saturated by a terminal hydrogen atom. The O–H distances are 1.0 Å, and the orientation of O–H bonds is along the pre-existing O–Si bonds. The clusters simulating the amine adsorption in HMOR are constructed by the partially optimized 20T cluster of HMOR and the free optimized amines. The amine molecules are put pointing to the 12-membered ring with the nitrogen atom closing to the acidic proton (H_z).

2.2. Methods

All the calculations in this work are performed by using the ONIOM2 method in the Gaussian 98 program. In the ONIOM2 framework, the system is divided into two layers and treated at two different levels of theory. In this work, the high-layer of the HMOR cluster contains two different models (2T and 6T, see Fig. 2) and is described by the B3LYP/6-31G(d,p) method. This large basis set including polarization function on hydrogen is used to describe the hydrogen bonding effectively. In the amines adsorption complexes (Fig. 3) the high-layer also includes the amine molecule. The rest of the cluster forming the low level layer is described by HF/3-21G. Four linking H atoms between the two layers are used to avoid the chemically unrealistic model and they replace four Si atoms in the cluster.

The 20T cluster representing the structure of HMOR are partially optimized with the acid site and its neighboring Si

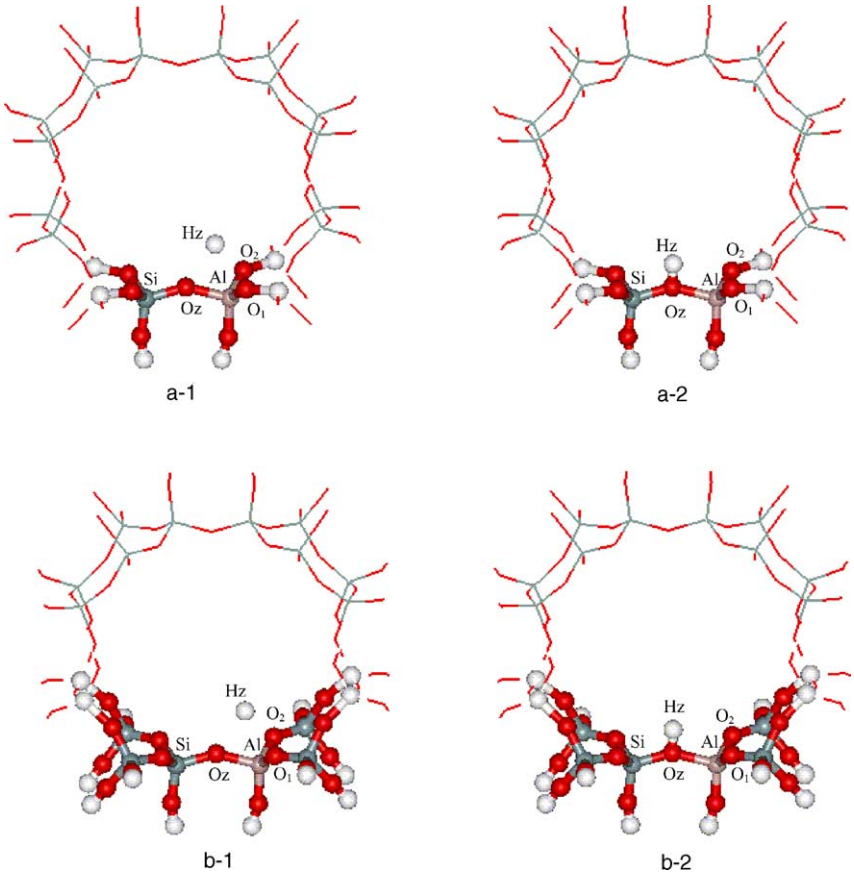

Fig. 2. The initial and optimized configuration of 20T models simulating the structure of HMOR (a) with 2T as high-layer (b) with 6T as high-layer.

and Al as well as the oxygen atoms surrounding Al relaxed, while the rest atoms are fixed to their crystal positions. This allows the atoms in the vicinity of the acid site to relax, while the cluster retains its position in the zeolite lattice. For the optimization of the adsorption complexes, the bond parameters of the adsorbate molecules and the atoms described above in the bare HMOR clusters are relaxed while the rest of the clusters are fixed.

To calculate IR frequencies of the adsorbed states, 6T models (see Fig. 4) are used which is cut from each optimized adsorption complexes with all the interaction atoms of the adsorbates and the zeolite framework included. Geometry optimizations and frequency calculations are performed at the B3LYP/6-31G(d) level.

3. Results and discussion

3.1. Comparison of models

In order to give a precise description on the adsorption of amines in HMOR with economical computer time, two kinds of 20T ONIOM2 models, with high-layer being 2T and 6T, respectively (see Fig. 2), are investigated, and the adsorption of amines are also investigated on these two models (see Fig. 3). To ensure all the interactions in the higher-layer, the 6T model of high-layer in $MeNH_2$ adsorption complex is different from others. Tables 1 and 2, respectively present the optimized bond lengths of the bare 20T clusters with 2T and 6T as high-layer and their amine adsorption complexes. It can be found that the difference in the Al–O bond lengths ($R_{Al–O_z}$, $R_{Al–O_1}$ and $R_{Al–O_2}$) and the distance between acidic proton and the bridging oxygen, $R_{H_z–O_z}$, between these two models is very small. By comparing the structure parameters of the two NH_3 complexes on HMOR, it is shown that the two models give the same NH_3 configuration: (i) NH_3 is protonated by the acidic proton on both clusters, (ii) NH_4^+ is more close to the oxygen atoms at Al than at Si, (iii) three hydrogen bonds are formed between hydrogen atoms of NH_4^+ and the oxygen atoms of the negatively charged zeolite framework. These results indicate that the 20T cluster with 2T as high-layer is enough for the study of NH_3 adsorption. However, for substituted amines such as $MeNH_2$, Me_2NH and Me_3N, the structure of the adsorption complexes shows some differences. Because C–H bonds can also interact with the framework oxygen atoms around the acid center, the smaller 2T model as high-layer becomes rather limited. Therefore, we take the 6T model as high-layer for our calculations at B3LYP/6-31G(d,p), and the results from 6T high-layer models are used for discussion.

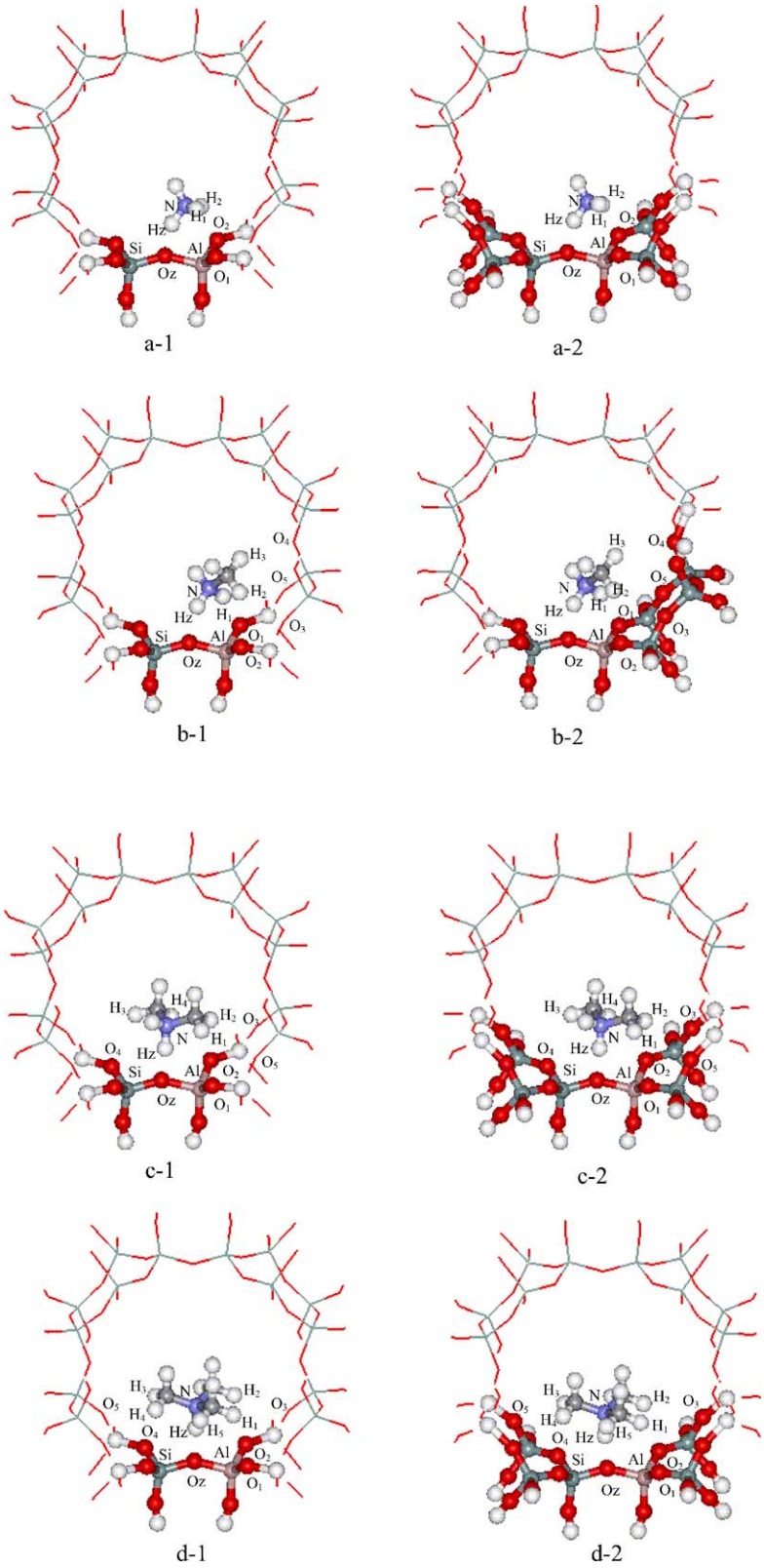

Fig. 3. Structures of the adsorption complexes of amines in 20T models with 2T and 6T as high-layer, respectively (a) NH_3 (b) $MeNH_2$ (c) Me_2NH (d) Me_3N.

Table 1
The selected bond lengths (Å) of the HMOR cluster and the amines adsorption complexes[a] in 20T model with 2T as higher layer

	20T	NH_3-20T	$MeNH_2$-20T	Me_2NH-20T	Me_3N-20T
$R_{O_z-H_z}$	0.978	1.584	1.826	1.557	1.531
R_{Al-O_z}	1.882	1.823	1.811	1.874	1.821
R_{Al-O_1}	1.719	1.778	1.767	1.770	1.756
R_{Al-O_2}	1.721	1.753	1.770	1.786	1.741
R_{N-H_z}	–	1.093	1.055	1.095	1.076
$R_{O_1-H_1(N)}$	–	2.408	1.768	–	–
$R_{O_1-H_1(N)}$	–	–	–	2.688	2.480
$R_{O_1-H_1(C)}$	–	2.037	–	–	–
$R_{O_2-H_2(N)}$	–	–	2.609	2.479	2.542
$R_{O_2-H_2(C)}$	–	–	2.595	2.623	2.792
$R_{O_3-H_2(C)}$	–	–	2.868	2.690	2.537
$R_{O_4-H_3(C)}$	–	–	2.927	–	–
$R_{O_5-H_1(C)}$ ($R_{O_5-H_3(C)}$)	–	–	–	2.889	(2.734)
$R_{O_2-H_4(C)}$ ($R_{O_4-H_4(C)}$)	–	–	–	2.794	(2.769)
$R_{O_z-H_5(C)}$	–	–	–	–	2.894

[a] The numbering of the atoms follows those designated in Figs. 2 and 3.

3.2. Structure of amine complexes

The configuration of the complexes with $MeNH_2$, Me_2NH, and Me_3N in HMOR is shown in Fig. 3, and the calculated bond lengths are listed in Table 2. From the distances between the acidic proton of HMOR and the bridging oxygen ($R_{O_z-H_z}$, 1.537–1.682 Å) and the nitrogen of amine molecules (R_{N-H_z}, 1.070–1.094 Å), it can be found that the proton has been transferred from the zeolite framework to the adsorbed amines and the ion-pair structure of $[ZeO^- \cdots {}^+HNR_3]$ is formed. The formed $[HNR_3]^+$ is stabilized by N–H···O and C–H···O hydrogen bonds through the negatively charged framework oxygens and the hydrogens of the amine and the methyl groups of the adsorbates, with O–H distances ranging from 1.537 to 2.889 Å.

As found in a previous paper [19] and the results discussed above, NH_4^+ forms three hydrogen bonds through its hydrogen atoms and the zeolite framework, including one strong ($R_{O_z-H_z}$, 1.586 Å) and two weaker ($R_{O_1-H_1}$, 2.554 Å; $R_{O_2-H_2}$, 1.923 Å) N–H···O interactions. For $MeNH_2$, Me_2NH and Me_3N molecules, one or more hydrogen atoms are replaced by methyl groups, producing molecules with larger size as compared with the parent ammonia molecule, and therefore more hydrogen atoms become closer to the framework oxygen atoms of the zeolite wall, leading to the formation of more than three hydrogen bonds in their complexes. Besides the interactions between lattice oxygen atoms and the hydrogen atoms bonded to nitrogen, the hydrogen atoms of the methyl groups also have interactions with zeolite lattice oxygen atoms. The strongest interaction is from the hydrogen atoms of the amine group in $[R_3NH]^+$ and the bridging lattice oxygen to aluminum, with the O–H distances ranging from 1.537 to 1.822 Å, while the interactions from hydrogen atoms of methyl groups

Table 2
The selected bond lengths (Å) of the HMOR cluster and the amines adsorption complexes[a] in 20T model with 6T as higher layer

	20T	NH_3-20T	$MeNH_2$-20T	Me_2NH-20T	Me_3N-20T
$R_{O_z-H_z}$	0.977	1.586	1.682	1.553	1.537
R_{Al-O_z}	1.884	1.826	1.815	1.845	1.805
R_{Al-O_1}	1.716	1.768	1.767	1.797	1.778
R_{Al-O_2}	1.752	1.788	1.769	1.757	1.747
R_{N-H_z}	–	1.100	1.070	1.094	1.080
$R_{O_1-H_1(N)}$	–	2.554	1.822	–	–
$R_{O_1-H_1(C)}$	–	–	–	2.691	2.487
$R_{O_2-H_2(N)}$	–	1.923	–	–	–
$R_{O_2-H_2(C)}$	–	–	2.507	2.495	2.410
$R_{O_3-H_2(C)}$	–	–	2.595	2.674	2.889
$R_{O_4-H_3(C)}$	–	–	2.849	2.678	2.535
$R_{O_5-H_3(C)}$	–	–	–	–	(2.599)
$R_{O_2-H_4(C)}$ ($R_{O_4-H_4(C)}$)	–	–	–	2.708	(2.690)
R_{N-H} (average)[b]	–	1.028 (1.018)	1.032 (1.017)	1.022 (1.017)	–
R_{C-N} (average)[b]	–	–	1.493 (1.465)	1.494 (1.457)	1.505 (1.455)
R_{C-H} (average)[b]	–	–	1.090 (1.098)	1.090 (1.099)	1.090 (1.099)

[a] The numbering of the atoms follows those designated in Figs. 2 and 3.
[b] The average lengths of all N–H, C–N or C–H bonds, respectively, in the adsorbed state, and the data in parentheses are the values of the free molecules.

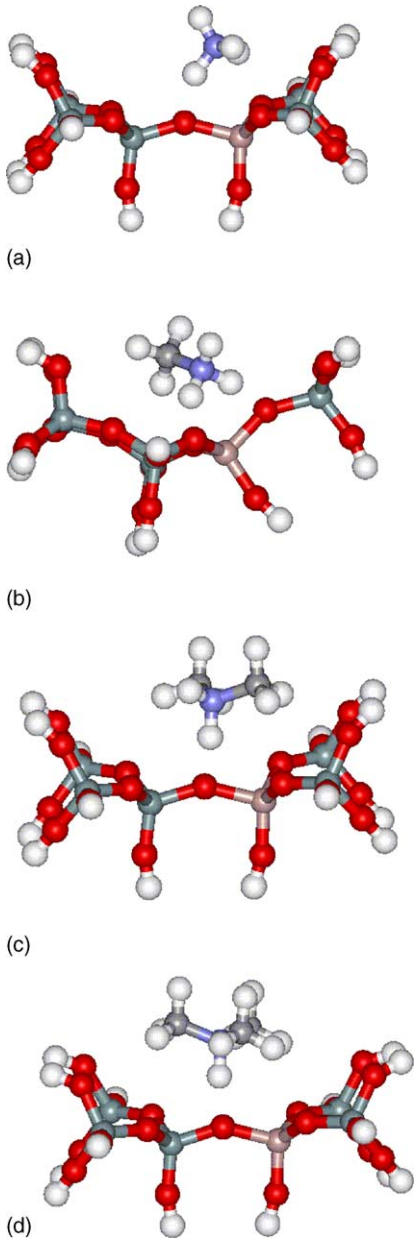

Fig. 4. The 6T cluster models used for frequency calculations of the adsorption complexes (a) NH_3 (b) $MeNH_2$ (c) Me_2NH (d) Me_3N.

are rather weaker with most of the O–H distances longer than 2.5 Å.

It is worth noting that in $MeNH_3^+$ adsorption complex there are two N–H bonds to interact with the zeolite framework oxygen atoms (with $R_{O–H}$ is 1.682 and 1.822 Å, Table 2), while only one in $Me_2NH_2^+$ and Me_3NH^+ (with $R_{O–H}$ is 1.553 and 1.537 for Me_2NH and Me_3NH complexes, respectively, Table 2). These double N–H···O hydrogen bonds in $MeNH_3^+$ result in the longer $R_{O–H}$ distance, as compared with that in $Me_2NH_2^+$ and Me_3NH^+.

As a result of these interactions, the Al–O_z distances become shorter than the bare cluster. The N–H and C–N bonds are elongated and the C–H bonds become shorter as compared with the free amines. From the structure of the adsorption complexes shown in Fig. 3 and the structure parameters presented in Table 2, it can be found that the main interactions between the adsorbates and the zeolite substrate are included in the high-layer of the ONIOM2 models, indicating that the models used in the present work are efficient in studying the adsorption of amine molecules in HMOR zeolites.

Table 3
Adsorption energies (kJ/mol) in the HMOR 20T cluster and proton affinities (PA; kJ/mol), compared with their experimental values and the corresponding pK_a of the conjugate acid of amines

	NH_3	$MeNH_2$	Me_2NH	Me_3N
ΔE_{ads} (calculated)[a]	136.9	161.1	198.3	187.1
ΔE_{ads} (calculated)[b]	135.6	157.3	191.0	186.2
ΔE_{ads} (experimental) [34–36]	160	200	225	220
PA (calculated) [43]	846.0	891.6	921.7	940.1
PA (experimental) [36,44]	858.3	896.4	923.2	939.1
pK_a [33]	9.3	10.6	10.7	9.7

[a] The adsorption energies calculated from 20T models with 2T as higher-layer.
[b] The adsorption energies calculated from 20T models with 6T as higher-layer.

3.3. Adsorption energies

The adsorption energy (ΔE_{ads}) is defined as the energy difference between the adsorption complexes and the two monomers (20T cluster and amine) and is calculated by: $\Delta E_{ads} = (E_{adsorbate} + E_{20T}) - E_{adsorbate-20T}$. Table 3 presented the calculated ΔE_{ads} for NH_3, $MeNH_2$, Me_2NH and Me_3N in HMOR. The proton affinity (PA) for the amines in gas phase is also listed in Table 3. It can be seen that in the gas phase, the order of the relative basicity of these amine molecules follows $NH_3 < MeNH_2 < Me_2NH < Me_3N$, due to the induction effect of alkyl groups. However, as measured by the pK_a of their conjugate acids [33] (Table 3), the basicity increases in the order: $NH_3 < Me_3N < MeNH_2 < Me_2NH$, which is resulted from the solvent effects. Here, when measured by their adsorption energies on acidic zeolites, the basicity of these amines increases as follows: $NH_3 < MeNH_2 < Me_3N < Me_2NH$, which is the same order as measured by experiments, [34–36], but different from the basicity order of in both the gas phase and solvents. The difference might be caused by the stabilization of the adsorbates by the zeolite framework and is related to their different molecular structures. When comparing our calculated adsorption energy of amines with the experimental results, however, it is found that our calculations underestimate the adsorption energy by 24–43 kJ/mol. This maybe due to that the B3LYP functional dose not account for dispersion forces [37–40].

3.4. IR frequencies

Frequency analysis is carried out on 6T clusters around the Oz center, cut from the partially optimized 20T adsorp-

Table 4
B3LYP/6-31G(d) stretching frequencies (cm^{-1}) of N–H and C–H bands of amines in the gas phase and adsorbed states[a]

	NH_3 (g)	NH_4^+ (g)	NH_4^+ (ads)	Shift (NH_4^+ (ads) − NH_4^+ (g))
N–H	3431, 3430, 3303	3351, 3349, 3348, 3233	3442, 3234, 3179, 2296	91, −115, −168, −936
	$MeNH_2$ (g)	$MeNH_3^+$ (g)	$MeNH_3^+$ (ads)	Shift ($MeNH_3^+$ (ads) − $MeNH_3^+$ (g))
N–H	3411, 3331	3344, 3343, 3261	3381, 2961, 2675	37, −382, −585
C–H	2998, 2960, 2855	3096, 3096, 3995	3087, 3064, 2982	−10, −32, −13
	Me_2NH (g)	$Me_2NH_2^+$ (g)	$Me_2NH_2^+$ (ads)	Shift ($Me_2NH_2^+$ (ads) − $Me_2NH_2^+$ (g))
N–H	3359	3334, 3283	3339, 2154	5, −1129
C–H	2997, 2996, 2951, 2950, 2833, 2826	3087, 3086, 3083 3083, 2988, 2986	3092, 3079, 3058 3057, 2969, 2960	– 5, −7, −25, −26, −19, −26
	Me_3N (g)	Me_3NH^+ (g)	Me_3NH^+ (ads)	Shift (Me_3NH^+ (ads) − Me_3NH^+ (g))
N–H	–	3298	2821	−476
C–H	2999, 2999, 2994, 2958, 2953, 2953, 2824, 2807, 2806	3079, 3079, 3079 3077, 3076, 3075 2985, 2981, 2980	3103, 3085, 3075, 3061, 3056, 3047, 2976, 2966, 2960	– 24, 6, −4, −16, −20, −28, −9, −15, −20

[a] All the frequencies presented here have been scaled by 0.9613.

tion models in which all the interactions are included, and these results are listed in Table 4. In order to analyze the interaction of the amines with the zeolite framework, it is necessary to compare the IR frequencies of free R_3N(g) and free R_3NH^+(g) in gas phase, and those of free R_3NH^+(g) and adsorbed R_3NH^+(ads).

As given in Table 4, NH_4^+(g) has lower N–H frequencies than NH_3(g) due to the charge effect, and the shifts are up to 80 cm^{-1}. The same trends are found for $MeNH_3^+$(g), $Me_2NH_2^+$(g) as compared to $MeNH_2$(g) and Me_2NH(g), but in less extent (ca. 70 and 25 cm^{-1}). These changes are in line with the elongated N–H bonds upon protonation (Table 2) and agree nicely with the experimental observation [41]. It is interesting to note that the C–H frequencies of R_3NH^+(g) are higher than R_3N(g), e.g. up to 67–140 cm^{-1} for $MeNH_3^+$(g), 90–160 cm^{-1} for $Me_2NH_2^+$(g) and 80–174 cm^{-1} for Me_3NH^+(g). These up-shifts can be ascribed to the absence of the negative hyperconjugation [42] of the nitrogen lone-pair in the protonated structures, and are in line with the elongation of the C–N bonds and the slightly shortening of the C–H bonds upon protonation (Table 2).

The strength of the interaction between R_3NH^+ and the zeolite framework can be estimated by comparing the N–H and C–H IR frequencies of R_3NH^+(g) and R_3NH^+(ads), as given in Table 4. The largest shifts are found for the $N–H_z$ bonds, which have strong hydrogen bonding to the bridging oxygen atom (O_z), e.g. down-shift of 936 cm^{-1} for NH_4^+(ads), 585 cm^{-1} for $MeNH_3^+$(ads), 1129 cm^{-1} for $Me_2NH_2^+$(ads) and 476 cm^{-1} for Me_3NH^+(ads). These changes agree with the variation of the $R_{O_z–H_z}$ and $R_{N–H_z}$ distances (Table 2). The shifts of the other hydrogen bonding are relatively small. When compared with the R_3NH^+(g), most of the C–H frequencies in the adsorbed states are shifted downward by small values, indicating that the interaction between the lattice oxygen atoms and C–H bonds are minor as compared with that of the N–H bonds.

4. Conclusions

The adsorption of four amines, NH_3, $MeNH_2$, Me_2NH, and Me_3N, in HMOR were investigated by the two-layered ONIOM computational method. It was shown that the amines are all protonated by the acidic proton of HMOR. In addition to the hydrogen bonding of hydrogen atoms on nitrogen and the negatively charged framework oxygen atoms, there is also weaker interaction between the methyl hydrogen atoms and the framework oxygen atoms (apart from NH_4^+). The N–H stretching frequencies of the adsorbed R_3NH^+ are computed to be up-shifted, as compared to those of the free protonated forms. In addition, the calculated adsorption energies agree reasonably with the experimental data. The basicity of the adsorbed amines differs from those in the gas phase (proton affinities) and in solution (pK_a values).

Acknowledgements

The authors are grateful to National Natural Science Foundation of China for the financial support (No. 20073057), and to the Alexander von Humboldt Foundation for the donation of computing facilities.

References

[1] B. Hunger, M. Heuchel, L.A. Clark, R.Q. Snurr, J. Phys. Chem. B 106 (2002) 3882.
[2] B. Onida, F. Geobaldo, F. Testa, R. Aiello, E. Garrone, J. Phys. Chem. B 106 (2002) 1684.

[3] S. Lim, G.L. Haller, J. Phys. Chem. B 106 (2002) 8437.
[4] Z.K. Xie, Q.L. Chen, C.F. Zhang, J.Q. Bao, Y.H. Cao, J. Phys. Chem. B 104 (2000) 2853.
[5] S. Bates, J. Dwyer, J. Phys. Chem. 97 (1993) 5897.
[6] A.M. Ferrari, K.M. Neyman, T. Belling, M. Mayer, N. Rosch, J. Phys. Chem. B 103 (1999) 216.
[7] P. Li, Y. Xiang, V.H. Grassian, S.C. Larsen, J. Phys. Chem. B 103 (1999) 5058.
[8] E.H. Teunissen, A.P.J. Jansen, R.A. van Santen, J. Chem. Phys. 101 (1994) 5865.
[9] A. Kyrlidis, S.J. Cook, A.K. Chakraborty, A.T. Bell, D.N. Theodorou, J. Phys. Chem. 99 (1995) 1505.
[10] J.M. Vollmer, E.V. Stefanovich, T.N. Truong, J. Phys. Chem. B 103 (1999) 9415.
[11] V.V. Mihaleva, R.A. van Santen, A.P.J. Jansen, J. Phys. Chem B 105 (2001) 6874.
[12] S.A. Zygmunt, R.M. Mueller, L.A. Curtiss, L.E. Iton, J. Mol. Struct. (TheoChem.) 430 (1998) 9.
[13] S. Bates, J. Dwyer, J. Mol. Struct.(TheoChem.) 306 (1994) 57.
[14] S.P. Greatbanks, I.H. Hillier, N.A. Burton, P. Sherwood, J. Chem. Phys. 105 (1996) 3770.
[15] A.G. Pelmenschikov, R.A. van Santen, J. Phys. Chem. 97 (1993) 10678.
[16] M. Stöcker, Micro. Meso. Mater. 29 (1999) 3.
[17] E.G. Derouane, J.G. Fripiat, in: Proceedings of the Sixth International Zeolite Conference, Reno, July 1983, paper no. 717.
[18] S.P. Yuan, J.G. Wang, Y.W. Li, S.Y. Peng, J. Mol. Catal. A 175 (2001) 131.
[19] S.P. Yuan, J.G. Wang, Y.W. Li, H. Jiao, J. Mol. Struct. 2004, ASAP online available.
[20] F. Docquir, V. Norberg, H. Toufar, J.-L. Paillaud, B.L. Su, Langmuir 18 (2002) 5963.
[21] F. Docquir, H. Toufar, B.L. Su, Langmuir 17 (2001) 6282.
[22] U. Eichler, M. Brändle, J. Sauer, J. Phys. Chem. B 101 (1997) 10035.
[23] M. Brändle, J. Sauer, J. Am. Chem. Soc. 120 (1998) 1556.
[24] R.Ch. Deka, K. Hirao, J. Mol. Catal. A 181 (2002) 275.
[25] F. Maseras, K. Morokuma, J. Comput. Chem. 16 (1995) 1170.
[26] S. Dapprich, I. Komáromi, K.S. Byun, K. Morokuma, M.J. Frisch, J. Mol. Struct. (TheoChem.) 461/462 (1999) 1.
[27] G.S. Tschumper, K. Morokuma, J. Mol. Struct. (TheoChem.) 592 (2002) 137.
[28] M.J. Frisch, G.W. Trucks, H.B. Schlegel, G.E. Scuseria, M.A. Robb, J.R. Cheeseman, V.G. Zakrzewski, J.A. Montgomery, Jr., R.E. Stratmann, J.C. Burant, S. Dapprich, J.M. Millam, A.D. Daniels, K.N. Kudin, M.C. Strain, O. Farkas, J. Tomasi, V. Barone, M. Cossi, R. Cammi, B. Mennucci, C. Pomelli, C. Adamo,S. Clifford, J. Ochterski, G.A. Petersson, P.Y. Ayala, Q. Cui, K. Morokuma, D.K. Malick, A.D. Rabuck, K. Raghavachari, J.B. Foresman, J. Cioslowski, J.V. Ortiz, A.G. Baboul, B.B. Stefanov, G. Liu, A. Liashenko, P. Piskorz, I. Komaromi, R. Gomperts, R.L. Martin, D.J. Fox, T. Keith, M.A. Al-Laham, C.Y. Peng, A. Nanayakkara, M. Challacombe, P.M.W. Gill,B. Johnson, W. Chen, M.W. Wong, J.L. Andres, C. Gonzalez,M. Head-Gordon, E.S. Replogle, J.A. Pople, Gaussian Inc., Pittsburgh, PA, 1998.
[29] H.-R. Tang, K.-N. Fan, Chem. Phys. Lett. 330 (2000) 509.
[30] I. Roggero, B. Civalleri, P. Ugliengo, Chem. Phys. Lett. 341 (2001) 625.
[31] X. Solans-Monfort, J. Bertran, V. Branchadell, M. Sodupe, J. Phys. Chem. B 106 (2002) 10220.
[32] M.M.J. Treacy, J.B. Higgins, R. von Ballmoos, Zeolites 16 (1996) 751.
[33] F.A. Carey, Organic Chemistry, McGraw-Hill, New York, 2003, p. 920.
[34] D.J. Parrillo, R.J. Gorte, W.E. Farneth, J. Am. Chem. Soc. 115 (1993) 12441.
[35] C. Lee, D.J. Parrillo, R.J. Gorte, W.E. Farneth, J. Am. Chem. Soc. 118 (1996) 3262.
[36] R.J. Gorte, D. White, Top. Catal. 4 (1997) 57.
[37] J.Šponer.J. Leszczynski, P. Hobza, J. Comput. Chem. 17 (1996) 841.
[38] L.A. Clark, M. Sierka, J. Sauer, J. Am. Chem. Soc. 12 (2003) 2136.
[39] A.M. Vos, X. Sierka, R.A. Schoonheydt, R.A. Van Santer, F. Hutschke, J. Hafner, J. Am. Chem. Soc. 123 (2001) 2799.
[40] X. Rozanska, R.A. Van Santen, F. Hutschka, J. Hafner, J. Am. Chem. Soc. 123 (2001) 7655.
[41] M. Hesse, H. Meier, B. Zeeh, Spektrosche Methoden in der Organische Chemie, 3. Auflage, Georg Thieme Verlag Stuttgart, 1987.
[42] P.v.R. Schleyer, A.J. Kos, Tetrahedron 39 (1983) 1141.
[43] H. Jiao, J.-F. Halet, J.A. Gladysz, J. Org. Chem. 66 (2001) 3902.
[44] R.S. Drago, T.R. Cundari, D.C. Ferris, J. Org. Chem. 54 (1989) 1042.